Wu *et al. EURASIP Journal on Wireless Communications and Networking* (2016) 2016:153
DOI 10.1186/s13638-016-0656-7

EURASIP Journal on Wireless Communications and Networking

RESEARCH Open Access

Maximum likelihood detection for coded combinerless LINC-OFDM systems

Wen-Rong Wu[1], Sheng-Lung Cheng[1*] and Ying-Pei Hsu[2]

Abstract

Owning to the high peak-to-average power ratio problem, the power efficiency of orthogonal-frequency-division-multiplexing (OFDM) systems is usually low. It deteriorates in millimeter wave systems in which the design of an efficient linear power amplifier is much more challenging. The linear-amplification-with-nonlinear-component (LINC) technique can serve as a remedy, decomposing the input signal into two constant-envelop component signals followed by high-efficient nonlinear amplifiers. However, the power combiner, a key component used to combine the amplified signals, is difficult to implement. Combinerless LINC systems employ two transmit antennas such that two component signals can be naturally combined at the receiver. Unfortunately, the performance of combinerless LINC-OFDM systems is seriously degraded if difference, even small, exists between the two channels. The maximum likelihood (ML) receiver can effectively solve the problem; however, its computational complexity is prohibitedly high. We propose a coded combinerless LINC-OFDM system, including a convolutional encoder and a list Viterbi algorithm (LVA) decoder, to solve the problem. The LVA can provide a small number of candidates for the ML detector, dramatically reducing the required computational complexity. We also utilize an enhanced zero-forcing equalizer such that the soft-demapping operation can be effectively conducted. Finally, we propose a simple iterative interference cancellation scheme to further enhance the performance. Simulations show that the proposed combinerless LINC-OFDM system can outperform the conventional OFDM while the consumed power is much lower.

Keywords: Linear-amplification-with-nonlinear-component (LINC), Orthogonal-frequency-division-multiplexing (OFDM), Peak-to-average power ratio (PAPR), Maximum likelihood (ML), List Viterbi algorithm (LVA)

1 Introduction

As known, power amplifier (PA) is the most power-hungry device in wireless transceivers. The PA efficiency heavily depends on the peak-to-average power ratio (PAPR) of the transmit signal. By allocating the modulated symbols on orthogonal subcarriers, orthogonal-frequency-division-multiplexing (OFDM) can have higher spectral efficiency and lower equalization complexity than conventional single-carrier systems [1]. For these reasons, OFDM has been widely adopted in today's wireless systems. However, combining of multiple modulated signals results in high-variant signal amplitude, yielding the high PAPR problem. A high PAPR signal requires a large PA power back-off, resulting in low PA efficiency. Recently, millimeter wave (mmWave) communication has been considered as a promising technology for future fifth-generation (5G) systems [2]. However, the PAPR problem will become even worse in mmWave systems. Designing high-linearity mmWave PAs remains a big challenge even with today's technology [3, 4].

In order to reduce the PAPR of the OFDM signal, some baseband signal processing methods, like amplitude clipping and filtering [5, 6], partial transmit sequence (PTS) [7, 8], coding [9], and selected mapping (SLM) [10], have been proposed. These methods can reduce the PAPR to some extent with the price of higher processing complexity or data redundancy. Another useful approach is to modify the architecture of RF signal amplification such that the linearity or the power efficiency can be enhanced [11–16].

Conventional transmitters use Cartesian modulation to form complex transmit signal. As a result, linear amplification is required, yielding large back-off for high PAPR

*Correspondence: sean0902.cm00g@nctu.edu.tw
[1] Institute of Communications Engineering, National Chiao Tung University, University Road, 30010 Hsinchu, Taiwan
Full list of author information is available at the end of the article

signal. Polar modulation, decomposing the complex transmit signal into amplitude and phase signals, allows the application of two different amplifications for the two signals. In the envelope-elimination-and-restoration (EER) transmitter [12], the phase signal (constant-enveloped) is amplified by a high-efficiency nonlinear PA and the amplitude signal by a linear PA. Then, the amplified amplitude signal is used to modulate the amplified phase signal, yielding the original signal amplified by an equivalent high-efficiency linear PA. Another polar transmission technique is known as envelope tracking (ET) [13] in which the amplitude signal is used to control the supply voltage of a linear PA such that the PA can always be operated in the high-efficiency regions. With a different operation principle, the Doherty transmitter [14] combines two equal-capacity PAs, referred to as carrier and peaking, in the quarter-wavelength network. Only the carrier PA is active when the amplitude of the signal is lower than the half of the peak amplitude, and both PAs are active when the signal amplitude is larger than the half of the peak amplitude. In the above approaches, the transmit signal is decomposed into two amplified by two PAs and there exist various kinds of implementation issues. For example, signal bandwidth is expanded and the stringent timing alignment between two signals is difficult. Still, there is another well-known approach referred to as linear-amplification-with-nonlinear-component (LINC) technique [17] to be described in the next paragraph.

In the LINC transmitter (also called as the outphasing in [18]), the modulated signal is passed to a signal component separator (SCS) [17, 19] and then decomposed to two constant-envelope component signals. Since the two component signals are both constant-enveloped, they can be amplified by high-efficiency nonlinear PAs. After the amplification, the two component signals are then combined by a power combiner to obtain a linearly amplified signal. Figure 1 shows the block diagram of a LINC system. There are two main problems in the LINC system. The first one is that the two signal paths cannot be perfectly balanced and the combined signal will be distorted. Several methods for solving the PA imbalanced problem were discussed in [20, 21]. The second problem is the performance of the combiner. For good combining linearity, the matched combiner is generally used. However, the matched combiner will induce the severe power loss for high PAPR signals. Simulation results in [22] show that the power efficiency of the LINC transmitter with the matched power combiner is similar to that of the conventional transmitter without LINC. In [23], a multilevel LINC architecture which can increase the efficiency of the matched combiner was proposed. In [24], the Chireix combiner was proposed. By adding the shunt resistors and the transmission line coupler after both PAs, the power efficiency can be improved [22, 24]. However, the linearity of this design is degraded. This approach trades the linearity for the power efficiency.

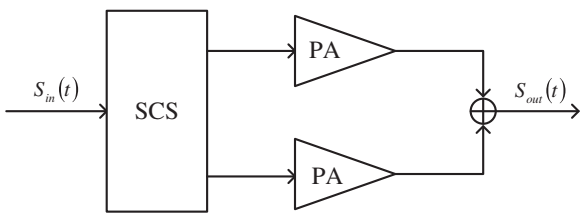

Fig. 1 Generic LINC architecture

To solve the problems of the conventional LINC, a combinerless LINC-OFDM system (CL-LINC-OFDM) was then developed [25]. With two closed-spaced antennas for signal transmission, the use of the power combiner can be avoided. Two component signals can be naturally combined in the air and received at the destination. Simulation results in [25] show that the efficiency of the combinerless LINC system is about 6 dB higher than the LINC system with the matched combiner. An experimental demonstration of the combinerless LINC system was also shown in [26]. However, the performance of the CL-LINC-OFDM system will be seriously affected if there is difference, even small, between the channels that the two component signals propagate. This effect is critical but not considered in [25]. To overcome, a space-time coded combinerless LINC system was proposed in [27]. The price to pay for this approach is that the transmission rate is reduced by half. Yet, a beamforming outphasing system was proposed in [28]. Still, the throughput will be affected when the phase error of the beamforming is considered. In our previous work [29], an enhanced equalization method is proposed using the LINC property, but its performance is still far away from the conventional OFDM system. In [30] , several suboptimum ML detection methods for the CL-LINC-OFDM were proposed, reducing the computational complexity to some extent. It was shown that with the ML detection, LINC-OFDM can have similar performance as conventional OFDM. However, the computational complexity is still far too high for real-world applications.

In this paper, we propose a coded CL-LINC-OFDM system to solve the problems in [30]. In the system, a convolutional channel encoder is introduced and a specially-designed Viterbi (VA) algorithm, referred to as the list VA (LVA) is applied at the receiver. The main idea is that with LVA, the number of candidates considered in the likelihood calculation is dramatically reduced and the computational complexity of the ML detector can be reduced to a realizable level. We also utilize the enhanced equalization method in [29] such that better soft input

for the LVA can be obtained. Finally, we propose a simple iterative interference cancellation (IC) method that can further enhance the performance of the proposed CL-LINC-OFDM system. Simulations show that the proposed CL-LINC-OFDM system can outperform the conventional OFDM while the consumed power is much lower. The remainder of this paper is organized as follows. The second section describes the system model, the problems of CL-LINC-OFDM systems, and existing solutions. The third section describes the equalizer that we use. The fourth section shows the proposed ML detection with the LVA. The fifth section analyses the power efficiencies of conventional OFDM and CL-LINC-OFDM systems. The sixth section provides simulation results to evaluate the performance of the proposed algorithms, and the seventh section gives conclusions.

2 System model

Figure 2 shows the block diagram of the proposed coded CL-LINC-OFDM system. In the figure, $\mathbf{d} = [d_0, \ldots, d_{N-1}]^T$ denotes a length-N bit sequence to be transmitted with an OFDM symbol. With the channel encoding and symbol mapping operations, $\mathbf{d}$ is transferred to a frequency-domain OFDM symbol denoted as $\mathbf{s} = [s_0, \ldots, s_{M-1}]^T$, where M is the number of subcarriers. Then, $\mathbf{s}$ is passed through the inverse-discrete-Fourier-transform (IDFT) operation, and the output is expressed by $\mathbf{s}_t = [s_{t,0}, \ldots, s_{t,M-1}]^T$. Note that $\mathbf{s}_t$ does not include the cyclic prefix (CP). The SCS [19] decomposes $\mathbf{s}_t$ into two constant-envelope component symbols denoted as

$$\mathbf{s}_{t1} = \frac{\mathbf{s}_t}{2} + \mathbf{e} = [s_{t1,0}, \ldots, s_{t1,M-1}]^T, \tag{1}$$

and

$$\mathbf{s}_{t2} = \frac{\mathbf{s}_t}{2} - \mathbf{e} = [s_{t2,0}, \ldots, s_{t2,M-1}]^T, \tag{2}$$

where

$$\mathbf{e} = \left[j\frac{s_{t,0}}{2}\sqrt{\frac{V_0^2}{|s_{t,0}|^2} - 1}, \ldots, j\frac{s_{t,M-1}}{2}\sqrt{\frac{V_0^2}{|s_{t,M-1}|^2} - 1} \right]^T. \tag{3}$$

In (3), V_0 is the peak magnitude for the OFDM signal. If any $|s_{t,i}|$ is larger than V_0, $|s_{t,i}|$ will be clipped and substituted by V_0, and the resultant component signal will be $\frac{V_0}{2} \cdot \frac{s_{t,i}}{|s_{t,i}|}$. The value of V_0 should be chosen as a compromise between the level of clipping noise and the magnitude of PAPR. If V_0 is large, the clipping noise will be small and the PAPR will be large and vice versa. Let the ith component of $\mathbf{s}_t$, $\mathbf{s}_{t1}$, and $\mathbf{s}_{t2}$ be denoted by $s_{t,i}$, $s_{t1,i}$, and $s_{t2,i}$, respectively. Figure 3 shows the relationship of $s_{t,i}$, $s_{t1,i}$, and $s_{t2,i}$. With CP added, $\mathbf{s}_{t1}$ and $\mathbf{s}_{t2}$ are delivered to nonlinear PAs and then transmitted by two closed-spacing antennas, TX_1 and TX_2. Denote the channel impulse responses between TX_1, TX_2 and the receiver as $\mathbf{h}_1 = [h_{1,0}, \ldots, h_{1,P-1}]^T$ and $\mathbf{h}_2 = [h_{2,0}, \ldots, h_{2,P-1}]^T$, respectively, where P is the number of the channel taps. For the channel corresponding to the same transmit antenna, we assume that each tap is statistically independent.

At the receiver, the CP of the received OFDM symbol is first removed and then an M-point DFT is applied. The received frequency-domain signal can then be written as

$$\mathbf{y} = \mathbf{H}_1\mathbf{s}_1 + \mathbf{H}_2\mathbf{s}_2 + \mathbf{n}, \tag{4}$$

where $\mathbf{n}$ is an $M \times 1$ additive white Gaussian noise (AWGN) vector with a covariance matrix of $\sigma_n^2\mathbf{I}$; $\mathbf{H}_1$ and $\mathbf{H}_2$ are two $M \times M$ diagonal matrices with diagonal elements being equal to the DFTs of $\mathbf{h}_1$ and $\mathbf{h}_2$, respectively; $\mathbf{s}_1$ and $\mathbf{s}_2$ are the DFTs of $\mathbf{s}_{t1}$ and $\mathbf{s}_{t2}$, respectively.

From the definitions of $\mathbf{s}_{t1}$ and $\mathbf{s}_{t2}$ in (1) and (2), we can simply see that $\mathbf{s} = \mathbf{s}_1 + \mathbf{s}_2$ since $\mathbf{s}_t = \mathbf{s}_{t1} + \mathbf{s}_{t2}$. We can also see that the CL-LINC-OFDM system is equal to the conventional OFDM system if $\mathbf{H}_1 = \mathbf{H}_2$. In real world, the

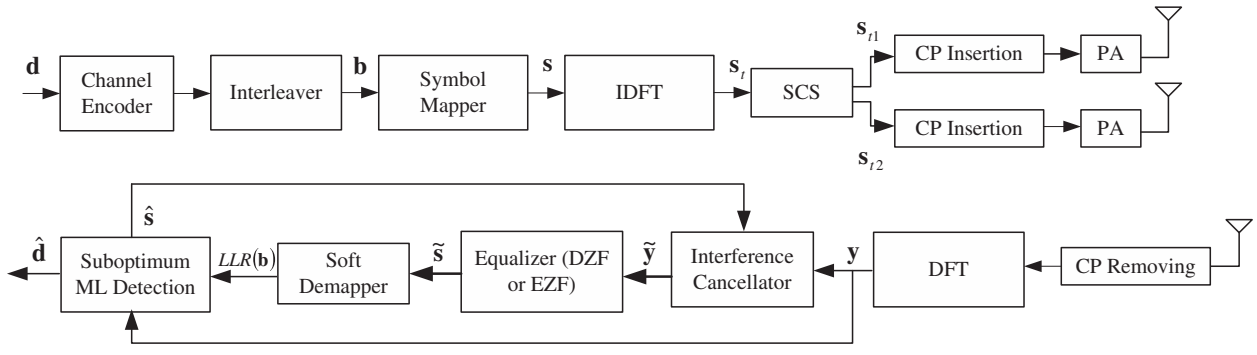

Fig. 2 The transmitter and receiver structure of the proposed coded CL-LINC-OFDM system

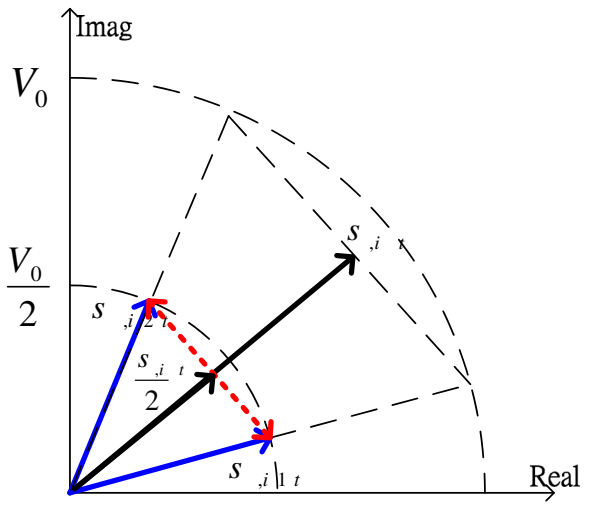

Fig. 3 The relationship between $s_{t,i}$, $s_{t1,i}$, and $s_{t2,i}$

two channel responses cannot be exactly the same, though they are close. We may simply assume that $\mathbf{H}_1 \approx \mathbf{H}_2$ and apply a zero-forcing (ZF) equalizer to recover $\mathbf{s}$. Let $\mathbf{H} = (\mathbf{H}_1 + \mathbf{H}_2)/2$ and $\hat{\mathbf{s}}$ be the ZF estimate of $\mathbf{s}$. Then, we have

$$\hat{\mathbf{s}} = \mathbf{H}^{-1}\mathbf{y}. \tag{5}$$

Unfortunately, it is found that the performance of CL-LINC-OFDM can be seriously degraded if there exists a difference between $\mathbf{H}_1$ and $\mathbf{H}_2$. This is because the channel difference will introduce a strong self-interference. For reference convenience, we refer the ZF equalizer in (5) as the direct ZF (DZF) equalizer.

In [27], the idea of space-time coding is applied in the CL-LINC-OFDM system to solve the problem. The Alamouti code is used in a way that for one symbol time $\mathbf{s}_{t1}$ and $\mathbf{s}_{t2}$ are transmitted by TX_1 and TX_2, respectively, and for the next symbol time, $-\mathbf{s}_{t2}^*$ and $\mathbf{s}_{t1}^*$ are transmitted. Using two consecutive received OFDM symbols and some simple operations, we can obtain two signals $\tilde{\mathbf{s}}_1$ and $\tilde{\mathbf{s}}_2$ as

$$\tilde{\mathbf{s}}_1 = (\mathbf{H}_1\mathbf{H}_1^H + \mathbf{H}_2\mathbf{H}_2^H)\mathbf{s}_1 + \mathbf{H}_1^H\mathbf{n}_1 + \mathbf{H}_2\mathbf{n}_2^*, \tag{6}$$

and

$$\tilde{\mathbf{s}}_2 = (\mathbf{H}_1\mathbf{H}_1^H + \mathbf{H}_2\mathbf{H}_2^H)\mathbf{s}_2 + \mathbf{H}_2^H\mathbf{n}_1 - \mathbf{H}_1\mathbf{n}_2^*, \tag{7}$$

where $\mathbf{n}_1$ and $\mathbf{n}_2$ are the noise vectors of the two consecutive OFDM symbols. From the above equations, it is simple to see that $\mathbf{s}$ can be recovered without any interference; the estimate of $\mathbf{s}$ is given by $(\mathbf{H}_1\mathbf{H}_1^H + \mathbf{H}_2\mathbf{H}_2^H)^{-1}(\tilde{\mathbf{s}}_1 + \tilde{\mathbf{s}}_2)$. However, the main drawback of this approach is that the throughput is reduced by half.

Except for the DZF method, the well-known ML method can also be applied to (4). Let the number of candidates for $\mathbf{s}$ be K, $\mathbf{s}^k$ be the kth candidate, and $\mathbf{s}_{1,k}$ and $\mathbf{s}_{2,k}$ be the two component signals of $\mathbf{s}^k$. The ML problem can then be formulated as:

$$\hat{k} = \arg \min_{1 \le k \le K} \|\mathbf{y} - (\mathbf{H}_1\mathbf{s}_{1,k} + \mathbf{H}_2\mathbf{s}_{2,k})\|^2. \tag{8}$$

It is readily to see that the computational complexity of (8) is prohibitedly high and the solution of (8) is almost impossible to obtain. Let the QAM size of each subcarrier be Q. Then, K will be equal to Q^M. For a simple OFDM system with QPSK modulation and 64 subcarriers, $K = 4^{64}$! Note that for each k, we have to conduct one DFT and one IDFT operations. The suboptimum solution proposed in [30] is to alleviate this problem; only the detected symbols (with the DZF method) considered to be unreliable are taken in the ML search. Also, the subcarriers are grouped and the ML search is only conducted for each individual group, sequentially. Let U be the number of unreliable detected symbols, G be the number of groups, and G divides U. Then, $K = GQ^{U/G}$. As an example, let $Q = 4$, $U = 12$, and $G = 3$. Then, we have $K = 3 \times 4^{12/3} = 768$. In other words, we have to conduct 768 DFTs/IDFTs for each OFDM symbol. Although the complexity has been significantly reduced, it is still too high for practical systems.

In the following sections, we will propose a new approach to overcome the ML detection problem in (8). The main idea is to include a convolutional code (CC) channel encoder in the transmitter. The CC encoder in our system serves two purposes. The first one, as that in a typical communication system, is to enhance the transmission reliability. The second one is to reduce the number of the candidates considered in the ML detection. For the channel decoder to operate, we first need QAM symbols to be detected softly. The ZF method mentioned in (5) can do the job. However, its performance is not satisfactory. In the following section, we will first propose an enhanced ZF equalizer and then the corresponding soft demapper.

3 Enhanced equalization method

In [29], we proposed an enhanced equalization method and we utilize it for the initial processing of the received CL-LINC-OFDM signal. To start with, we first reformulate the received signals in (4). Define a diagonal matrix $\mathbf{C}(\mathbf{s}_t)$ as

$$\mathbf{C}(\mathbf{s}_t) = \begin{bmatrix} \sqrt{\frac{V_0^2}{|s_{t,0}|^2} - 1} & 0 & \cdots & 0 \\ 0 & \sqrt{\frac{V_0^2}{|s_{t,1}|^2} - 1} & \cdots & 0 \\ \vdots & \vdots & \ddots & \vdots \\ 0 & 0 & \cdots & \sqrt{\frac{V_0^2}{|s_{t,M-1}|^2} - 1} \end{bmatrix}. \tag{9}$$

By (9) and the definition of $\mathbf{e}$ in (3), we can rewrite $\mathbf{s}_{t1}$ and $\mathbf{s}_{t2}$ as

$$\begin{aligned}\mathbf{s}_{t1} &= \left(\mathbf{I} + j\mathbf{C}(\mathbf{s}_t)\right)\frac{\mathbf{s}_t}{2}\\ \mathbf{s}_{t2} &= \left(\mathbf{I} - j\mathbf{C}(\mathbf{s}_t)\right)\frac{\mathbf{s}_t}{2},\end{aligned} \tag{10}$$

where $\mathbf{I}$ is an $M \times M$ identity matrix. The received signal in (4) can then be written as

$$\mathbf{y} = \frac{1}{2}\left(\mathbf{H}_1 + \mathbf{H}_2\right)\mathbf{s} + \frac{j}{2}\left(\mathbf{H}_1 - \mathbf{H}_2\right)\mathbf{F}\mathbf{C}(\mathbf{s}_t)\mathbf{F}^H\mathbf{s} + \mathbf{n}, \tag{11}$$

where $\mathbf{F}$ and $\mathbf{F}^H$ are used to denote the DFT and IDFT matrices; both of them are assumed to be unitary. Note that $\mathbf{s}_t = \mathbf{F}^H\mathbf{s}$. From (11), we can see that the original representation of the received signals has been transferred to a form in which $\mathbf{s}$ instead of $\mathbf{s}_1$ and $\mathbf{s}_2$ is involved. Also, we can see that if $\mathbf{H}_1$ is not equal to $\mathbf{H}_2$, the second term in the right-hand-side of (11) acts as an interference. The magnitude of this interference can be large even the difference of $\mathbf{H}_1$ and $\mathbf{H}_2$ is small, and this is the reason why CL-LINC-OFDM with DZF performs not well.

Observe that the diagonal terms in $\mathbf{C}(\mathbf{s}_t)$ are all greater or equal to zero which suggests that the means of these terms are not zero. If the non-zero-means can be removed, the level of the interference can be reduced. Define a positive value μ and rewrite (11) as

$$\begin{aligned}\mathbf{y} &= \frac{1}{2}\left(\mathbf{H}_1 + \mathbf{H}_2\right)\mathbf{s} + \frac{j}{2}\left(\mathbf{H}_1 - \mathbf{H}_2\right)\mathbf{F}\left[\mathbf{C}(\mathbf{s}_t) - \mu\mathbf{I} + \mu\mathbf{I}\right]\mathbf{F}^H\mathbf{s} + \mathbf{n}\\ &= \frac{1}{2}\left[\left(\mathbf{H}_1 + \mathbf{H}_2\right) + j\mu\left(\mathbf{H}_1 - \mathbf{H}_2\right)\right]\mathbf{s} + \frac{j}{2}\left(\mathbf{H}_1 - \mathbf{H}_2\right)\mathbf{F}\left(\mathbf{C}(\mathbf{s}_t)\right.\\ &\quad \left. - \mu\mathbf{I}\right)\mathbf{F}^H\mathbf{s} + \mathbf{n}.\end{aligned} \tag{12}$$

Then, the equalized symbols can be obtained as

$$\hat{\mathbf{s}} = 2\left[\left(\mathbf{H}_1 + \mathbf{H}_2\right) + j\mu\left(\mathbf{H}_1 - \mathbf{H}_2\right)\right]^{-1}\mathbf{y}. \tag{13}$$

When μ is equal to zero, (13) is reduced to (5). So, (13) can be seen as a generalized form of the DZF equalizer when CL-LINC-OFDM transmission is applied. We name this equalizer as the enhanced ZF (EZF) equalizer.

The performance of the EZF equalizer strongly depends on the choice of μ. We now derive an optimum μ such that the average power of the interference is minimized. Define a vector $\mathbf{v}$ as

$$\mathbf{v} = \left[\mathbf{C}(\mathbf{s}_t) - \mu\mathbf{I}\right]\mathbf{s}_t. \tag{14}$$

Thus, the interference vector in (12) is equal to $\frac{j}{2}\left(\mathbf{H}_1 - \mathbf{H}_2\right)\mathbf{F}\mathbf{v}$. To calculate the variance of the interference in each subcarrier, we first calculate that of $\mathbf{v}$. When M is large, it is reasonable to approximate $\mathbf{s}_t$ as a zero-mean complex white Gaussian vector. The covariance matrix of $\mathbf{s}_t$ can be expressed as $E_s\mathbf{I}$ where E_s is the power of the transmit signal. The mean of each component of $\mathbf{v}$ is given by

$$E\left\{\left(\sqrt{\frac{V_0^2}{|s_{t,i}|^2} - 1} - \mu\right)s_{t,i}\right\} = E\left\{s_{t,i}\sqrt{\frac{V_0^2}{|s_{t,i}|^2} - 1}\right\}. \tag{15}$$

Note that $s_{t,i}$ is a zero-mean complex Gaussian random variable such that $s_{t,i}\sqrt{\frac{V_0^2}{|s_{t,i}|^2} - 1}$ and $-s_{t,i}\sqrt{\frac{V_0^2}{|-s_{t,i}|^2} - 1}$ have the same appearing probability, and the expectation value of (15) is zero. By the truth that each element of $\mathbf{v}$ is also independent to each other, the covariance matrix of $\mathbf{v}$ can be seen as an $M \times M$ diagonal matrix with the same diagonal term. Defining each diagonal term as σ_v^2 and assuming $\frac{V_0^2}{E_s} \gg 1$, we can approximate $|s_{t,i}|$ as a Rayleigh distributed random variable and its probability density function (PDF) is given by

$$p\left(|s_{t,i}|\right) = \frac{2|s_{t,i}|}{E_s}e^{\frac{-|s_{t,i}|^2}{E_s}}. \tag{16}$$

The value of σ_v^2 can then be derived as

$$\begin{aligned}\sigma_v^2 &= E\left\{\left|\left(\sqrt{\frac{V_0^2}{|s_{t,i}|^2} - 1} - \mu\right)s_{t,i}\right|^2\right\}\\ &= E\left\{|s_{t,i}|^2\left(\frac{V_0^2}{|s_{t,i}|^2} - 1\right)\right\} - 2\mu E\left\{|s_{t,i}|^2\sqrt{\frac{V_0^2}{|s_{t,i}|^2} - 1}\right\}\\ &\quad + \mu^2 E\left\{|s_{t,i}|^2\right\}\\ &= V_0^2 + \left(\mu^2 - 1\right)E_s - 2\mu E\left\{|s_{t,i}|^2\sqrt{\frac{V_0^2}{|s_{t,i}|^2} - 1}\right\}.\end{aligned} \tag{17}$$

To derive a closed-form solution for the third term of (17), we use an approximation that $\sqrt{1-x} \approx 1 - 0.6x$:

$$\begin{aligned}|s_{t,i}|^2\sqrt{\frac{V_0^2}{|s_{t,i}|^2} - 1} &= |s_{t,i}|V_0\sqrt{1 - \frac{|s_{t,i}|^2}{V_0^2}}\\ &\approx V_0|s_{t,i}|\left(1 - 0.6\frac{|s_{t,i}|^2}{V_0^2}\right)\\ &= V_0|s_{t,i}| - 0.6\frac{|s_{t,i}|^3}{V_0}.\end{aligned} \tag{18}$$

The approximation used in (18) is modified from the first-order Taylor expansion such that better performance can be obtained. With the PDF shown in (16), the mean and the third moment of $|s_{t,i}|$ can be obtained as

$$E\left\{|s_{t,i}|\right\} = \frac{\sqrt{E_s\pi}}{2}, \text{ and } E\left\{|s_{t,i}|^3\right\} = \frac{3\sqrt{\pi}}{4}E_s^{\frac{3}{2}}. \tag{19}$$

Substituting (18) and (19) to (17), we can obtain

$$\begin{aligned}\sigma_v^2 &\approx V_0^2 + \left(\mu^2 - 1\right) E_s - 2\mu E \left\{ V_0 |s_{t,i}| - 0.6 \frac{|s_{t,i}|^3}{V_0} \right\} \\ &= V_0^2 + \left(\mu^2 - 1\right) E_s - \mu V_0 \sqrt{E_s \pi} + \frac{0.9\mu\sqrt{\pi}}{V_0} E_s^{\frac{3}{2}} \\ &= V_0^2 - E_s - \frac{1}{4} E_s \left(V_0 \sqrt{\frac{\pi}{E_s}} - \frac{0.9\sqrt{\pi E_s}}{V_0} \right)^2 \\ &\quad + E_s \left[\mu - \frac{1}{2} \left(V_0 \sqrt{\frac{\pi}{E_s}} - \frac{0.9\sqrt{\pi E_s}}{V_0} \right) \right]^2. \end{aligned} \tag{20}$$

Equation (20) is a quadratic function of μ, and the optimum μ giving the smallest σ_v^2 can be easily found as:

$$\mu = \frac{V_0}{2} \sqrt{\frac{\pi}{E_s}} - \frac{0.45\sqrt{\pi E_s}}{V_0}. \tag{21}$$

The corresponding σ_v^2 can also be obtained as

$$\begin{aligned}\sigma_v^2 &= V_0^2 - E_s - \frac{1}{4} E_s \left(V_0 \sqrt{\frac{\pi}{E_s}} - \frac{0.9\sqrt{\pi E_s}}{V_0} \right)^2 \\ &= V_0^2 \left[\left(1 - \frac{\pi}{4}\right) + (0.45\pi - 1) \frac{E_s}{V_0^2} - \frac{0.81\pi E_s^2}{4V_0^4} \right]. \end{aligned} \tag{22}$$

Since the channel encoder is operated on the bit level, the equalized symbol $\hat{\mathbf{s}}$ has to be de-mapped into soft bits, a process referred to as soft-demapping [31]. Soft-demapping for OFDM systems requires to calculate the log-likelihood-ratio (LLR) for each transmit bit. To do that, we have to first calculate the signal-to-interference-noise ratio (SINR) of the equalized signal at each subcarrier. Let the channel magnitude response of subcarrier k be G_k, and the variance of interference-plus-noise in the same subcarrier be σ_k^2. Then, the SINR, denoted as γ_k, can be calculated as:

$$\gamma_k = \frac{E_s |G_k|^2}{\sigma_k^2}. \tag{23}$$

As mentioned, the covariance matrix of $\mathbf{v}$ is diagonal. Then, the covariance matrix of the interference-and-noise vector in (12) is also diagonal and its kth diagonal term is given by

$$\begin{aligned}\sigma_k^2 &= \frac{|H_{1,k} - H_{2,k}|^2}{4} \sigma_v^2 \\ &\quad + \frac{|\left(H_{1,k} + H_{2,k}\right) + j\mu \left(H_{1,k} - H_{2,k}\right)|^2}{4} \sigma_c^2 + \sigma_n^2, \end{aligned} \tag{24}$$

where $H_{1,k}$ is the kth diagonal component of $\mathbf{H}_1$, $H_{2,k}$ is that of $\mathbf{H}_2$, σ_v^2 is the interference variance given in (22), and σ_c^2 is the variance of the clipping noise. From (22), we see that the value of σ_v^2 is an increasing function of V_0. Note that the value of V_0 determines the PAPR of the transmit signal. A smaller V_0 means a lower PAPR, higher power efficiency, and lower interference in (12). However, more signal samples will be clipped, increasing the

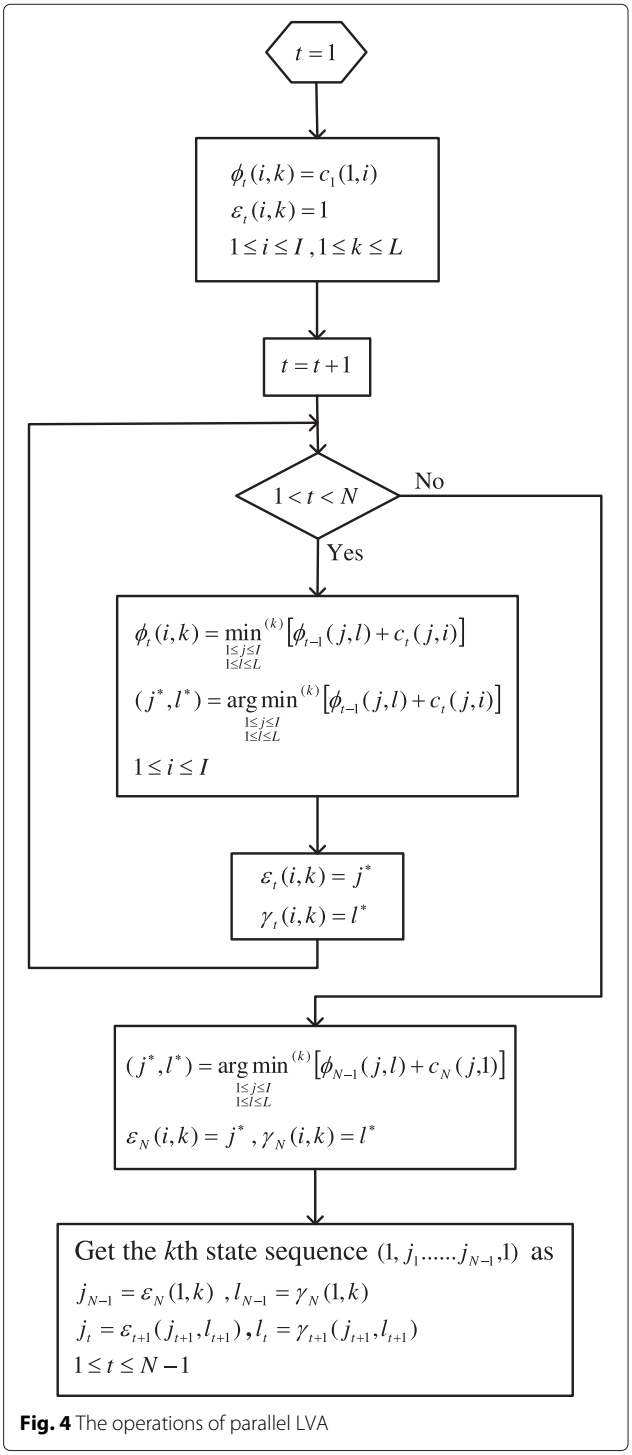

Fig. 4 The operations of parallel LVA

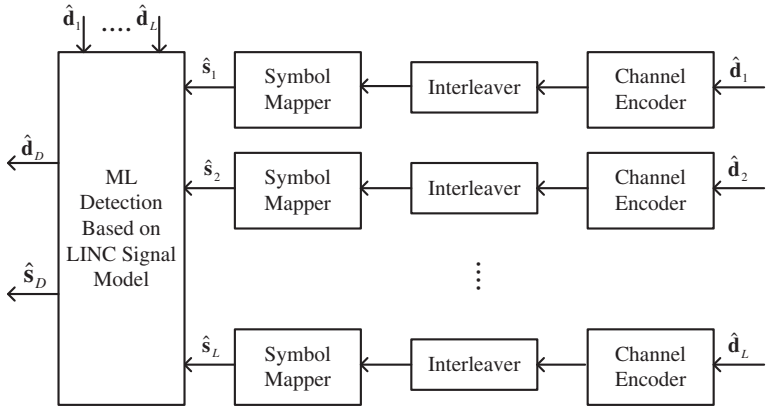

Fig. 5 The operations of ML detection in CL-LINC-OFDM system

clipping noise level. From (12), we can obtain the channel magnitude response and then calculate γ_k as

$$\gamma_k = \frac{A_c^2 E_s |\left(H_{1,k} + H_{2,k}\right) + j\mu\left(H_{1,k} - H_{2,k}\right)|^2}{\sigma_v^2 |H_{1,k} - H_{1,k}|^2 + \sigma_c^2 |\left(H_{1,k} + H_{2,k}\right) + j\mu\left(H_{1,k} - H_{2,k}\right)|^2 + 4\sigma_n^2}, \tag{25}$$

where A_c is an equivalent amplitude after clipping. The values of σ_c^2 and A_c can be found as follows. Denote the clipped time-domain OFDM signal as $\check{s}_{t,i}$ and the clipping ratio, equivalent to the square root of the PAPR value, as

$$\kappa = \frac{V_0}{\sqrt{E_s}}. \tag{26}$$

Since the time-domain OFDM symbol is approximated by a complex white Gaussian process, then

$$E\{|\check{s}_{t,i}|^2\} = E_s\left(1 - e^{-\kappa^2}\right). \tag{27}$$

In [32], it was shown that the clipped signal can be modelled as

$$\check{s}_{t,i} = A_c s_{t,i} + n_{c,i}, \tag{28}$$

where $n_{c,i}$ is a clipping noise uncorrelated to $s_{t,i}$. The value of A_c and the variance of $n_{c,i}$, denoted as σ_c^2, are found to be

$$A_c = 1 - e^{-\kappa^2} + \frac{\sqrt{\pi}\kappa}{2}\mathrm{erfc}\left(\kappa\right), \tag{29}$$

where erfc(.) denotes the complementary error function, and

$$\begin{aligned}\sigma_c^2 &= E\{|\check{s}_{t,i}|^2\} - A_c^2 E_s \\ &= E_s\left[1 - e^{-\kappa^2} - \left(1 - e^{-\kappa^2} + \tfrac{\kappa\sqrt{\pi}}{2}\mathrm{erfc}\left(\kappa\right)\right)^2\right] \\ &\approx E_s\left[e^{-\kappa^2} - \kappa\sqrt{\pi}\mathrm{erfc}\left(\kappa\right)\right].\end{aligned} \tag{30}$$

Finally, the LLR of the ith bit transmitted at kth subcarrier is obtained as

$$LLR\left(b_{i,k}\right) \approx \ln\frac{\max\limits_{\alpha\in S_{i,k}^1} P\left(\tilde{y}_k|s_k=\alpha\right)}{\max\limits_{\alpha\in S_{i,k}^0} P\left(\tilde{y}_k|s_k=\alpha\right)} = \gamma_k\{\min_{\alpha\in S_{i,k}^0}|\hat{s}_k-\alpha|^2 - \min_{\alpha\in S_{i,k}^1}|\hat{s}_k-\alpha|^2\}, \tag{31}$$

where $S_{i,k}^1$ or $S_{i,k}^0$ indicates the symbol set in which the ith bit of each element is 1 or 0. The LLR values are deemed as the de-mapped soft bits and then used as the input to the channel decoder.

As we can see from (30), the SINR at each subcarrier depends on the clipping ratio, κ. If κ is larger, the clipping noise will be smaller. At the same time, however, the interference will become stronger. We now derive a closed-form expression for the average SINR such that an optimum κ maximizing the average SINR can be found. Let the mean of each channel gain in $\mathbf{H}_1$ and $\mathbf{H}_2$ be normalized to one. Then, the average channel gain for the EZF can be obtained as

$$E\{|\left(H_{1,k} + H_{2,k}\right) + j\mu\left(H_{1,k} - H_{2,k}\right)|^2\} = 2 + 2\rho + 2\mu^2(1-\rho), \tag{32}$$

where $\rho = E\{H_{1,k}H_{2,k}^*\}$ denotes the antenna correlation. Substituting (20), (26), (30), and (32) into (25) and taking the expectation, we can obtain the average SINR (i.e., $E\{\gamma_k\}$), denoted by SINR_a, of the CL-LINC-OFDM system with the EZF equalizer as

$$\mathrm{SINR}_a = \frac{\bar{\rho}\left[1 - e^{-\kappa^2} + \frac{\sqrt{\pi}\kappa}{2}\mathrm{erfc}\left(\kappa\right)\right]^2}{(1-\rho)\left(\kappa^2 + \mu^2 + \frac{0.9\mu\sqrt{\pi}}{\kappa} - \kappa\mu\sqrt{\pi} - 1\right) + \bar{\rho}\left[e^{-\kappa^2} - \kappa\sqrt{\pi}\mathrm{erfc}\left(\kappa\right)\right] + 2\mathrm{SNR}^{-1}}, \tag{33}$$

where SNR=E_s/σ_n^2 and $\bar{\rho} = \left[1+\rho+\mu^2(1-\rho)\right]$. Using the value of μ in (21), we can rewrite the average SINR as

$$\mathrm{SINR}_a = \frac{\tilde{\rho}\left[1-e^{-\kappa^2}+\frac{\sqrt{\pi}\kappa}{2}\mathrm{erfc}(\kappa)\right]^2}{(1-\rho)\left[\kappa^2\left(1-\frac{\pi}{4}\right)+0.45\pi-1-\frac{0.81\pi}{4\kappa^2}\right]+\tilde{\rho}\left[e^{-\kappa^2}-\kappa\sqrt{\pi}\mathrm{erfc}(\kappa)\right]+2\mathrm{SNR}^{-1}}, \tag{34}$$

where $\tilde{\rho} = \left[1+\rho+\pi\left(\frac{\kappa}{2}-\frac{0.45}{\kappa}\right)^2(1-\rho)\right]$. As we can see, the average SINR is a function of ρ and κ. It can be shown that the average SINR is a concave function of κ. For each ρ, we can then find the optimum κ by a simple numerical search.

4 Maximum likelihood detection with list Viterbi algorithm

In this section, we would consider the architecture of the decoder. As mentioned, the decoder serves two purposes: one is for the reduction of the bit-error-rate and the other is to reduce the computational complexity of the ML detector. We first reconsider the LINC-OFDM system shown in (11). Re-arrange (11) as $\mathbf{y} = \tilde{\mathbf{H}}\mathbf{s} + \mathbf{n}$ where $\tilde{\mathbf{H}}$ is an $M \times M$ equivalent channel matrix given by

$$\tilde{\mathbf{H}} = \frac{1}{2}(\mathbf{H}_1+\mathbf{H}_2) + \frac{j}{2}(\mathbf{H}_1-\mathbf{H}_2)\,\mathbf{F}\mathbf{C}(\mathbf{s}_t)\mathbf{F}^H. \tag{35}$$

Since the diagonal terms in the diagonal matrix $\mathbf{C}(\mathbf{s}_t)$ are not all the same, the second term in (35) is not a diagonal matrix. It indicates that we cannot apply the carrier-by-carrier detection scheme as that in the conventional OFDM system. To have a better performance, we can apply the block-wise ML detection scheme as shown in (8). Unfortunately, as mentioned, the high computational complexity makes the general ML detection almost impossible to conduct. Here, we propose using the LVA [33] to reduce the number of candidates in the ML detection.

The LVA was originally proposed to enhance the performance of a concatenated coding system where the CC is used as the inner code. Since it is generally difficult to implement the joint decoding of both inner and outer codes, the inner code is softly decoded and the output is then used as the input for the outer decoder. Although the optimum decoding algorithm such as BCJR [34] can be applied, the required computational complexity is high. The LVA serves as an alternative soft decoding scheme by giving multiple decoded bit sequences. The conventional VA outputs a bit sequence while the LVA outputs multiple. With more input sequences, the reliability of the outer decoding can be enhanced. Simulation results in [33] verify that the performance of the concatenated coded system is indeed enhanced with the LVA. Here, we extend the use of the LVA to reduce the complexity of our ML problem.

Now, we briefly describe the operations of the LVA. The LVA can be implemented as parallel or sequential processing fashion. Since the outputs of these two kinds of LVAs are the same, we only discuss the parallel LVA here. The difference between the LVA and the VA lies in that the LVA reserves multiple while the VA only one survival path for each state. Let the number of states in the trellis be I and the number of survivor paths to preserve be L, the branch metric from state j to state i at time $(t-1)$ to t be $c_t(j,i)$, $c_t(j,i) = \infty$ when state i and j are not connected in the trellis diagram, and $\phi_t(i,k)$ be the kth lowest path metric to state i at time t. Figure 4 gives the detailed operations of the parallel LVA. Here, $\varepsilon_t(i,k)$ and $\gamma_t(i,k)$ denote the state and the corresponding ranking which can reach $\phi_t(i,k)$ at time $(t-1)$. Also, $\min^{(k)}(.)$ is the kth smallest value in the elements of (.). With the LVA, we can then obtain L state sequences having the lowest path metrics. For the lth state sequence, we can derive its detected bits from the corresponding two consecutive states as $\hat{\mathbf{d}}_l = \left[\hat{d}_{l,0}, \hat{d}_{l,1}, \ldots, \hat{d}_{l,N-1}\right]^T$.

Once we have the L best detected bit sequences, we can use them as the candidates for the block-wise ML detection. By this way, the number of the candidates can be dramatically reduced. Figure 5 shows the procedure of our low-complexity ML detector. Note that we have to regenerate the L best estimated symbol sequences, denoted by $\hat{\mathbf{s}}_1, \ldots \hat{\mathbf{s}}_L$, and each symbol sequence has to be re-encoded, re-interleaved, and symbol re-mapped. With the IDFT operation, we can obtain the L time-domain estimated

Table 1 Power efficiency comparison

PAPR (dB)	μ_{OFDM} (PA in [35]) (%)	μ_{LINC} (PA in [35]) (%)	μ_{LINC} (PA in [36]) (%)
6	2.25	9.19	15.15
8	1.42	5.82	9.59
10	0.9	3.68	6.07

Table 2 Simulation parameters

Parameters	Value
Number of FFT points (M)	128
CP length	16
Fading	Rayleigh fading
Channel tap number (P)	6
Power delay profile	Uniform power delay profile
Modulation	QPSK
Channel estimation	Ideal

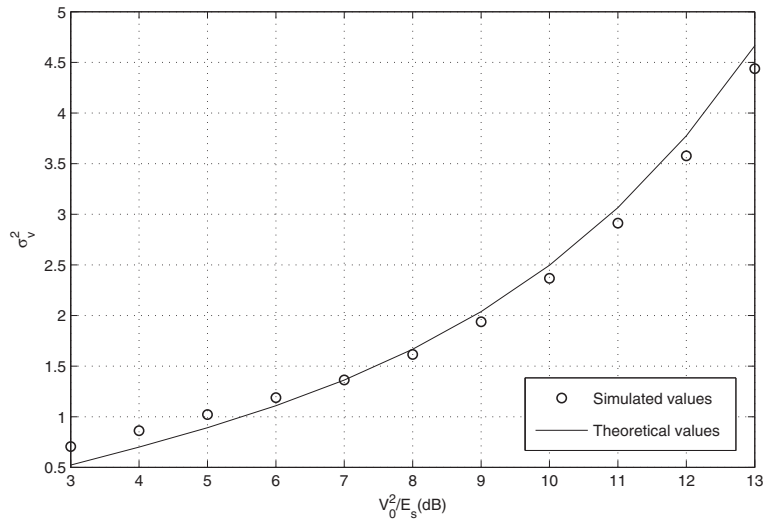

Fig. 6 Comparison of simulated σ_v^2 and theoretical σ_v^2 in (22)

OFDM symbols, denoted them as $\hat{\mathbf{s}}_{t,1},\ldots.\hat{\mathbf{s}}_{t,L}$. From (9) and (11), we can then obtain the ML detection from the L candidates as

$$\hat{l} = \arg \min_{1\le l\le L} \|\mathbf{y} - \frac{1}{2}(\mathbf{H}_1 + \mathbf{H}_2)\hat{\mathbf{s}}_l - \frac{j}{2}(\mathbf{H}_1 - \mathbf{H}_2)\mathbf{F}\mathbf{C}(\hat{\mathbf{s}}_{t,l})\mathbf{F}^H\hat{\mathbf{s}}_l\|. \quad (36)$$

Finally, the detected bit sequence can be obtained as $\hat{\mathbf{d}}_D = \hat{\mathbf{d}}_{\hat{l}}$.

To further enhance the performance, we now propose a simple IC method. As seen from (12), the second term is the interference when the EZF is applied. Let the ML detected symbol be $\hat{\mathbf{s}}_D$ and $\hat{\mathbf{s}}_{D,t} = \mathbf{F}^H\hat{\mathbf{s}}_D$. We can then use $\mathbf{C}(\hat{\mathbf{s}}_{D,t})$ to artificially generate the interference term and then conduct IC as

$$\tilde{\mathbf{y}} = \mathbf{y} - \xi\frac{j}{2}(\mathbf{H}_1 - \mathbf{H}_2)\mathbf{F}\left(\mathbf{C}(\hat{\mathbf{s}}_{D,t}) - \mu\mathbf{I}\right)\mathbf{F}^H\hat{\mathbf{s}}_D, \quad (37)$$

where ξ is a cancellation factor and $\xi < 1$. Note that we only conduct partial IC in order to control the error propagation effect. With $\tilde{\mathbf{y}}$, we can then apply the EZF equalizer, the LVA, and the ML detector again. This process can be repeated until a desired number of the iterations is met. The best partial cancellation factor ξ can be determined by simulations. In general, its value can be increased as the iteration proceeds since the detected symbols would become more and more reliable. When the IC scheme is applied, the SINR with the EZF equalization in (25) must be re-calculated. This can be obtained by

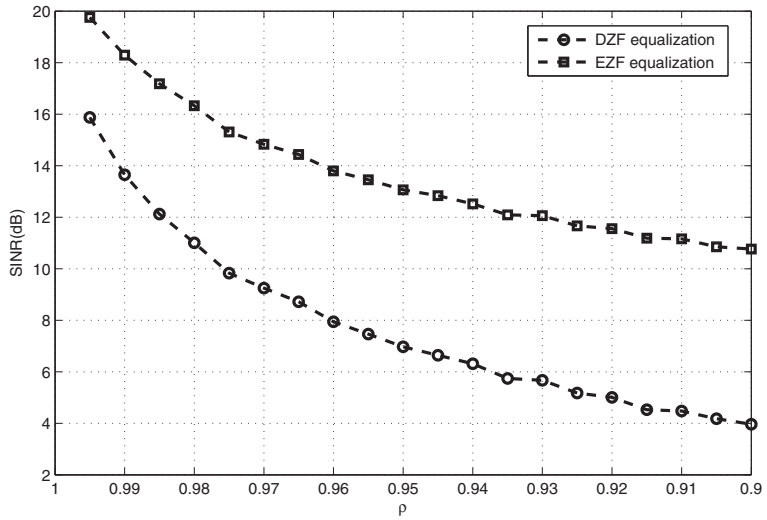

Fig. 7 Performance comparison of DZF and EZF equalizers in CL-LINC-OFDM systems (different antenna correlations)

$$\gamma_k = \frac{A_c^2 E_s |\left(H_{1,k} + H_{2,k}\right) + j\mu\left(H_{1,k} - H_{2,k}\right)|^2}{(1-\xi)^2\sigma_v^2 |H_{1,k} - H_{1,k}|^2 + \sigma_c^2 |\left(H_{1,k} + H_{2,k}\right) + j\mu\left(H_{1,k} - H_{2,k}\right)|^2 + 4\sigma_n^2}, \tag{38}$$

where the detected symbols are simply assumed to be all correct. With the SINR, the LLR can be re-calculated as that in (31).

5 Power efficiency of CL-LINC-OFDM systems

In this section, we analyze the power efficiency of the conventional OFDM and CL-LINC-OFDM systems. For conventional OFDM, only the linear PA is considered. For CL-LINC-OFDM, either linear or nonlinear PAs can be used. The input signal is assumed to be in its back-off range, and clipping is conducted for signal with amplitude exceeding the range. Let the maximum and the average output power of the transmitter be denoted by $P_{\max}$ and P_{out}, respectively. Then, $P_{\max} = V_0^2$ for OFDM systems. By assuming that PAs can be operated with approximately full linearity under $P_{1\,\text{dB}}$, the PA output power will only have 1 dB loss. Thus, we can have $P_{1\,\text{dB}} \approx P_{\max}$. The average power efficiency of the conventional OFDM system can be denoted by μ_{OFDM}, as [11]

$$\mu_{\text{OFDM}} = \frac{P_{\text{out}}}{P_{\text{in}}}, \tag{39}$$

where P_{in} means the average DC-input power. Since the conventional OFDM system is operated with linear PA (class A), the DC-input power is fixed [11] and can be written as

$$P_{\text{in}} = \frac{P_{1\,\text{dB}}}{\mu_{1\,\text{dB}}}, \tag{40}$$

where $\mu_{1\,\text{dB}}$ is the efficiency when the output power is $P_{1\,\text{dB}}$. Substituting (40) to (39), we can rewrite μ_{OFDM} as

$$\mu_{\text{OFDM}} = \frac{\mu_{1\text{dB}} P_{\text{out}}}{P_{1\,\text{dB}}} = \frac{\mu_{1\text{dB}} P_{\text{out}}}{P_{\max}} = \frac{\mu_{1\,\text{dB}}}{\text{PAPR}}. \tag{41}$$

For CL-LINC-OFDM, $P_{\max} = 2 \times V_0^2/4 = V_0^2/2$. Note that P_{out} of the CL-LINC-OFDM system is the average power after signal combining. Since the component signals are constant-enveloped, the PA can operate in its maximum efficiency which is denoted as $\mu_{\max}$. We then have the power efficiency of the CL-LINC-OFDM system, denoted by μ_{LINC}, as

$$\mu_{\text{LINC}} = \mu_{\max}\frac{P_{\text{out}}}{P_{\max}} = 2\frac{\mu_{\max}}{\text{PAPR}}. \tag{42}$$

Note here that the PAPR in (42) is the PAPR before signal separation. Specific figures for $\mu_{1\,dB}$ and $\mu_{\max}$ depend on the PA design. For comparison purposes, we choose the recent results in [35, 36] for the efficiency calculation. Here, the power efficiency μ is approximated as the power-added efficiency (PAE) for simplicity. For the linear PA in [35], $\mu_{1\,\text{dB}} = 9\,\%$ and $\mu_{\max} = 18.3\,\%$. For the nonlinear one (class AB) in [36], $\mu_{\max} = 30.3\,\%$. The efficiency of the conventional OFDM and CL-LINC-OFDM

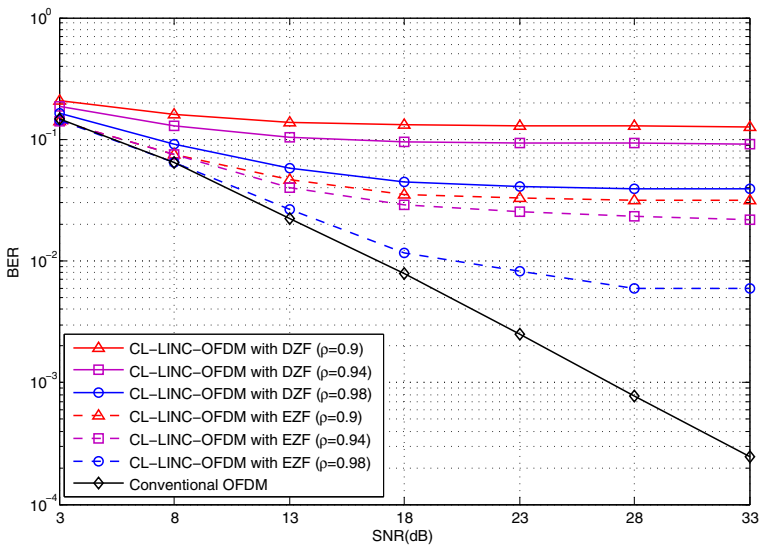

Fig. 8 Performance comparison of conventional OFDM and CL-LINC-OFDM systems (different antenna correlations)

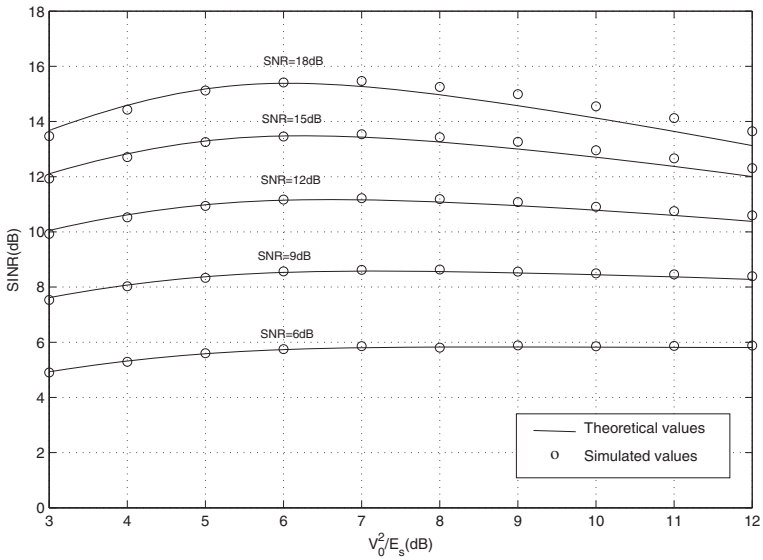

Fig. 9 Relationship of average SINR and PAPR in proposed CL-LINC-OFDM system

systems is then evaluated for PAPR being equal to 6, 8, and 10 dB, respectively. Table 1 shows the results calculated from (41) and (42). As we can see, the power efficiency of the CL-LINC-OFDM system is about four-time higher than that of the conventional OFDM system when the linear PA in [35] is applied. Similar result is also observed in [25, 26]. The power efficiency of the CL-LINC-OFDM system becomes about seven-time higher than that of the conventional OFDM system when the nonlinear PA in [36] is applied. The power efficiency of the CL-LINC-OFDM system can be even higher when PAs with higher nonlinearity are considered [4].

6 Simulation results

In this section, we report simulation results demonstrating the effectiveness of the proposed approaches. Table 2 gives the detailed simulation parameters.

We first evaluate the validity of the derived interference variance in (22) when the EZF is applied. Without loss of generality, we let $E_s = 1$. Figure 6 shows the simulated and the theoretical σ_v^2 for various V_0^2/E_s's. As we can see, the calculated values in (22) are close to the simulated results and the approximation error can be ignored.

We then evaluate the performance of the CL-LINC-OFDM system with the proposed EZF equalizer. A

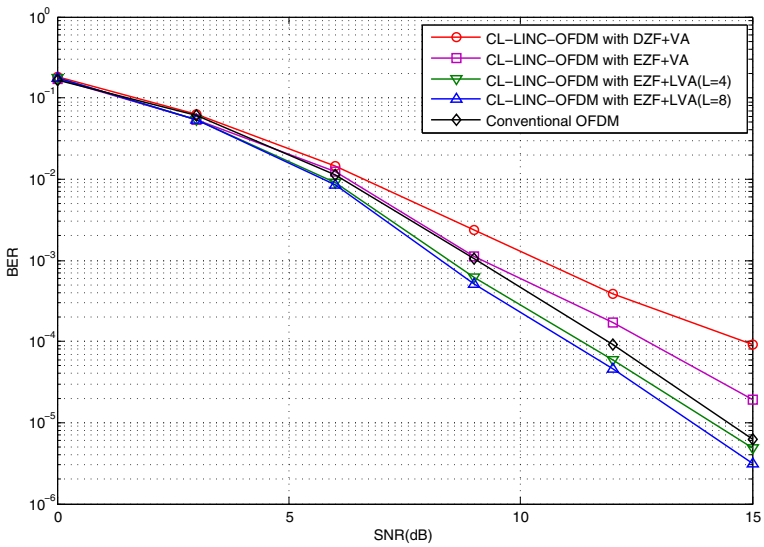

Fig. 10 Performance comparison of conventional coded OFDM system and proposed coded CL-LINC-OFDM system ($\rho = 0.98$)

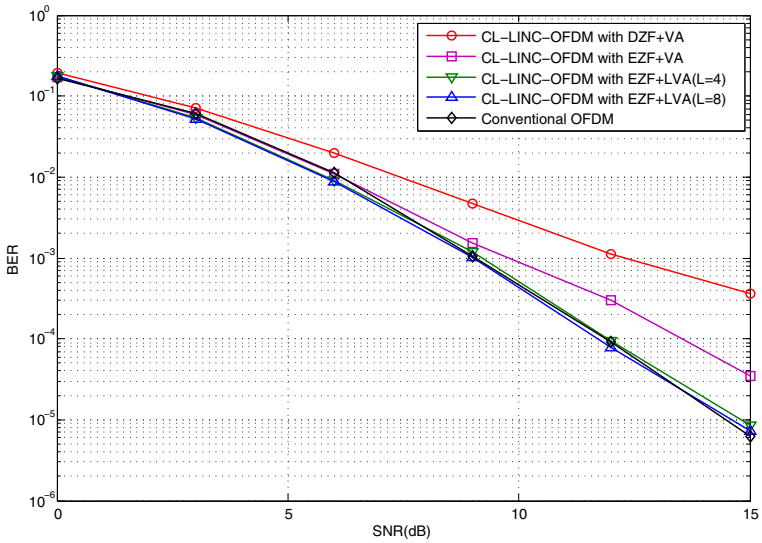

Fig. 11 Performance comparison of conventional coded OFDM system and proposed coded CL-LINC-OFDM system ($\rho = 0.96$)

channel model characterized by the antenna correlation is used in the simulations. Let $\mathbf{h}_p = \begin{bmatrix} h_{1,p} & h_{2,p} \end{bmatrix}^T$ be the vector consisting of the two pth taps of two channels. Denote its correlation matrix as $\mathbf{R}_p$. Then,

$$\mathbf{R}_p = E\left[\mathbf{h}_p \mathbf{h}_p^H\right] = P_p \begin{bmatrix} 1 & \rho \\ \rho & 1 \end{bmatrix}, \tag{43}$$

where P_p is the power of the pth tap and ρ is the correlation coefficient. With $\mathbf{R}_p$, we can generate the correlated MIMO channels. For details, see [37]. Since TX_1 and TX_2 are located closely, the two channel responses are highly correlated, which means ρ is close to one. When $\rho = 1$, $\mathbf{H}_1$ and $\mathbf{H}_2$ are fully correlated, i.e., $\mathbf{H}_1 = \mathbf{H}_2$ and the CL-LINC-OFDM system will be reduced to a conventional OFDM system. $\mathbf{H}_1$ and $\mathbf{H}_2$ are assumed to be known and the average SINR is used as the performance measure. Also, let $E_s/\sigma_n^2 = 20$ dB and PAPR = 10 dB. With this PAPR setting, the effect of the clipping noise can be neglected. For the conventional DZF equalizer, we have the average SINR, denoted by SINR_{DZF}, as

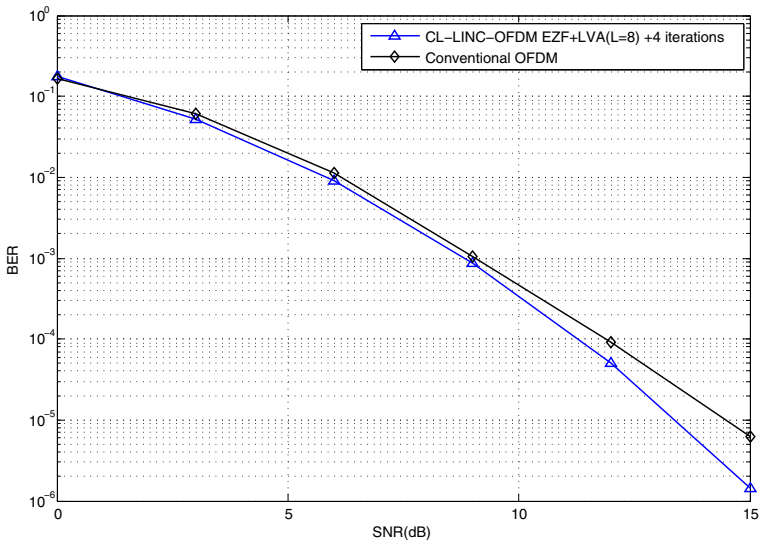

Fig. 12 Performance of proposed coded CL-LINC-OFDM system with interference cancellation ($\rho = 0.96$)

$$\mathrm{SINR}_{\mathrm{DZF}} = \frac{E\left\{\left|\left|\left(\frac{\mathbf{H}_1+\mathbf{H}_2}{2}\right)\mathbf{s}\right|\right|^2\right\}}{E\left\{\left|\left|\mathbf{y}-\left(\frac{\mathbf{H}_1+\mathbf{H}_2}{2}\right)\mathbf{s}\right|\right|^2\right\}}. \quad (44)$$

For the EZF equalizer, we have the average SINR, denoted by $\mathrm{SINR}_{\mathrm{EZF}}$, as

$$\mathrm{SINR}_{\mathrm{EZF}} = \frac{E\left\{\left|\left|\left(\frac{\mathbf{H}_1+\mathbf{H}_2}{2}+j\mu\frac{\mathbf{H}_1-\mathbf{H}_2}{2}\right)\mathbf{s}\right|\right|^2\right\}}{E\left\{\left|\left|\mathbf{y}-\left(\frac{\mathbf{H}_1+\mathbf{H}_2}{2}+j\mu\frac{\mathbf{H}_1-\mathbf{H}_2}{2}\right)\mathbf{s}\right|\right|^2\right\}}. \quad (45)$$

We evaluate the SINRs corresponding to different antenna correlations; Fig. 7 shows the simulation result. From the figure, we can see that the SINR is strongly affected by the antenna correlation. The smaller the correlation, the lower the SINR. For the DZF equalizer, the SINR is reduced from 16 to 4 dB when the correlation varies from 0.995 to 0.9. For the EZF equalizer, the SINR is reduced from 20 to 10.5 dB. As we can see, the EZF equalizer is much better than the DZF. Figure 8 shows the bit-error-rate (BER) simulations for various antenna correlations. As we can see, the EZF equalizer significantly outperforms the DZF equalizer. From Fig. 8, we can also see that the performance of the CL-LINC-OFDM is much worse than that of the conventional OFDM, especially when the antenna correlation is lower.

As we mentioned in the second section, the interference power depends on the value of V_0, i.e, the PAPR value. A smaller V_0 will result in a smaller interference level but a larger clipping noise level. Thus, there is an optimum V_0, i.e., an optimum clipping ratio. Simulations are then used to find the value. Figure 9 shows the relationship between SINR and PAPR when the EZF equalization is applied for $\rho = 0.98$. Note that the theoretical SINR derived in (34) is also shown. From Fig. 9, we can see that for higher SNR (for example, 15 dB), the optimum PAPR is between 6 and 7 dB. This result indicates that when PAPR is higher than 7 dB, the interference dominates the SINR, and when it is smaller than 6 dB, the clipping noise dominates. It can also be seen that the theoretical SINR is close to the simulated SINR.

From Fig. 9, we can also see that when input SNR is lower, the optimum clipping ratio tends to be higher. However, the variation of the resultant equalized SINR is small. It is then proper to let the optimum clipping ratio be 6 dB for all cases.

Now, we consider the proposed coded CL-LINC-OFDM system. We use a simple (2,1,2) CC encoder with the generator polynomials given by $g^{(1)} = 1 + D + D^2$ and $g^{(2)} = 1 + D^2$. For simplicity, we let the size of the coding block be 126. Then, the size of the coded output block will be $2 \times (126 + 2) = 256$ where the two additional bits are for tail bits. Without any puncturing, we can then fit each coded block into one QPSK OFDM symbol with size of $M = 128$. Also let the interleaver be a 16×16 block interleaver.

We now compare the performance of the conventional coded OFDM and the proposed coded CL-LINC-OFDM systems. For the both systems, the PAPR is set as 6 dB. The standard VA is used for the decoding scheme of the conventional OFDM while the proposed ML detector with the EZF equalizer is used for the proposed coded CL-LINC-OFDM system. The performance of the CL-LINC-OFDM system with conventional VA and DZF is also evaluated. Here, we use the performance of the conventional coded OFDM system as a benchmark. Figures 10 and 11 show the simulation results for $\rho = 0.98$ and $\rho = 0.96$, respectively. Similar to the previous case, the performance of the combinerless system degrades as the ρ is reduced. However, the level of the degradation is not as severe as that in the uncoded case. From Figs. 10 and 11, we can see that when the proposed ML detector is applied, the performance of CL-LINC-OFDM can be enhanced even for $L = 4$ in the LVA. Note that in some cases, the performance of the CL-LINC-OFDM is even better than the conventional OFDM. This is because the LINC operation can be viewed as a coding process; it acts as an inner code added for the system. With the inner code, the performance of CL-LINC-OFDM can outperform conventional OFDM. Figure 12 shows the simulation result when the IC scheme proposed in fourth section is applied. We let the number of iterations be three and ξ_i be the cancellation factor in the ith iteration. With simulations, we derive that $\xi_1 = 0.2$, $\xi_2 = 0.4$, and $\xi_3 = 0.8$. From the figure, we can see that CL-LINC-OFDM significantly outperforms conventional OFDM when SNR is higher (e.g., 15 dB). Note that we let $\rho = 0.96$ in the simulation case, implying that the performance gap will be even larger for $\rho = 0.98$.

7 Conclusions

In this paper, we propose a coded CL-LINC-OFDM system to solve the low power efficiency problem inherent in OFDM systems. First, we design an EZF equalizer that can have better performance in the combinerless system. Then, we use the LVA to obtain a small number of solution candidates such that the ML detection can be efficiently conducted for the CL-LINC-OFDM system. To further enhance performance, we develop a simple interference cancellation method. Simulation results show that the proposed coded CL-LINC-OFDM system can have the similar performance as the conventional OFDM. However, the power efficiency of the proposed CL-LINC-OFDM is much higher. When the antenna correlation is high enough, the proposed system can even have better performance than the conventional OFDM. Note that the CC decoder can be implemented with the BCJR algorithm

to provide soft outputs. How to use the soft outputs to obtain the ML solution deserves further investigations. As mentioned, the LINC operation can be seen as a coding process. How to calculate its soft outputs and apply sophisticate iterative decoding schemes can also serve potential topics for further research. Finally, a bandwidth problem needs to be considered for real-world applications. It is known that the bandwidth of the LINC component signals is much wider than its original signal. There are a number of methods to reduce the bandwidth, e.g., [38, 39]. However, these methods may distort the combined signal. How to recover the transmit signal at the receiver deserves further investigations. Research in these directions is now underway.

Competing interests
The authors declare that they have no competing interests.

Author details
[1]Institute of Communications Engineering, National Chiao Tung University, University Road, 30010 Hsinchu, Taiwan. [2]Mediatek Inc., Dusing 1st Rd, 30078 Hsinchu, Taiwan.

Received: 24 November 2015 Accepted: 14 June 2016
Published online: 29 June 2016

References

1. R van Nee, R Prasad, *OFDM for Wireless Multimedia Communications*, 1st edn. (Artech House, Boston, MA, 2000)
2. P Wang, Y Li, L Song, B Vucetic, Multi-gigabit millimeter wave wireless communications for 5G: from fixed access to cellular networks. IEEE Commun Mag. **53**(1), 168–178 (2015)
3. L Li, X Niu, L Chen, Y Chai, T Zhang, J Shi, *et al*, Design of 60GHz RF transceiver in CMOS: challenges and recent advances. China Commun. **11**(6), 32–41 (2014)
4. R Bhat, A Chakrabarti, H Krishnaswamy, in *IEEE MTT-s IMaRC 2014*. Advances in th Design of Efficient-yet-Linear Watt-Class mmWave CMOS, (Bangalore, India, 2014), pp. 53–56
5. J Armstrong, Peak-to-average power reduction for OFDM by repeated clipping and frequency domain filtering. Electronics Lett. **38**(5), 246–247 (2002)
6. X Zhu, W Pan, H Li, Y Tang, Simplified approach to optimized iterative clipping and filtering for PAPR reduction of OFDM signals. IEEE Trans Commun. **61**(5), 1891–1901 (2013)
7. SH Muller, JB Huber, OFDM with reduced peak-to-average power ratio by optimum combination of partial transmit sequences. Electronics Lett. **33**(5), 368–369 (1997)
8. L Li, D Qu, T Jiang, Partition optimization in LDPC-Coded OFDM systems with PTS PAPR reduction. IEEE Trans Veh Tech. **63**(8), 4108–4113 (2014)
9. AE Jones, TA Wilkinson, SK Barton, Block coding scheme for reduction of peak to mean envelope power ratio of multicarrier transmission schemes. Electronics Lett. **30**(25), 2098–2099 (1994)
10. RW Bauml, RFH Fischer, JB Huber, Reducing the peak-to-average power ratio of multicarrier modulation by selected mapping. Electronics Lett. **32**(22), 2056–2057 (1996)
11. FH Raab, P Asbeck, S Cripps, PB Kenington, ZB Popovic, N Pothecary, *et al*, Power amplifiers and transmitters for RF and microwave. IEEE Trans Microw Theory Tech. **50**(3), 814–826 (2002)
12. LR Kahn, Single-sideband transmission by envelope elimination and restoration. Proc IRE. **40**(7), 803–806 (1952)
13. C Buoli, A Abbiati, D Riccardi, in *Proc. 25th European Microwave Conf*. Microwave power amplifier with "envelope controlled" drain power supply, (Bologna, Italy, 1995), pp. 31–35
14. WH Doherty, A new high-efficiency power amplifier for modulated waves. Proc IRE. **15**(3), 469–475 (1936)
15. J Groe, Polar transmitters for wireless communications. IEEE Commun Mag. **45**(9), 58–63 (2007)
16. P Liang, H Wang, CH Peng, A Peng, HC Hwang, G Chien, *et al*, Digital transmitter design for mobile devices. IEEE Commun Mag. **51**(10), 114–123 (2013)
17. DC Cox, Linear amplification with nonlinear components. IEEE Trans Commun. **22**(12), 1942–1945 (1974)
18. H Chireix, High power outphasing modulation. Proc IRE. **23**(11), 1370–1392 (1935)
19. A Bateman, JP McGeehan, LINC transmitter. Electronics Lett. **27**(10), 844–846 (1991)
20. X Zhang, LE Larson, PM Asbeck, P Nanawa, Gain/phase imbalance-minimization techniques for LINC transmitters. IEEE Trans Microw. Theory Tech. **49**(12), 2507–2516 (2001)
21. L Sundstrom, Automatic adjustment of gain and phase imbalances in LINC transmitters. Electronics Lett. **31**(3), 155–156 (1995)
22. A Birafane, M El-Asmar, AB Kouki, M Helaoui, FM Ghannouchi, Analyzing LINC systems. IEEE Microwave Mag. **11**(5), 59–71 (2010)
23. KY Jheng, YJ Chen, AY Wu, Multilevel LINC system designs for power efficiency enhancement of transmitters. IEEE J Sel Top Signal Process. **3**(3), 523–532 (2009)
24. FH Raab, Efficiency of outphasing RF power-amplifier systems. IEEE Trans Commun. **33**(10), 1094–1099 (1985)
25. MA Elaal, *LINC Based Amplifier Architectures for Power Efficient Wireless Transmitters*. (Dept. Elect. Eng., Ecole Polytechnique De Montreal, Montreal, Canada, 2009)
26. F Benahmed Daho, G Neveux, M Mouhamadou, P Vaudon, C Decroze, D Carsenat, *An operational modified-LINC demonstrator for wireless communication*, (Rome, Italy, 2011), pp. 480–482
27. S Ali, B Adebisi, G Markarian, E Arikan, Signal combining in LINC amplifier using Alamouti codes. Electronics Lett. **46**(18), 1301–1302 (2010)
28. C Liang, B Razavi, Transmitter linearization by beamforming. IEEE J Solid-State Circ. **46**(9), 1956–1969 (2011)
29. SL Cheng, WR Wu, YP Hsu, *An enhanced zero-forcing equalizer for combinerless LINC-OFDM systems*, (Washington DC, USA, 2014), pp. 795–799
30. KS Hsu, in *Master thesis*. Maximum likelihood detection for combinerless LINC-OFDM systems (Inst. Commun. Eng., Nat. Chiao Tung Univ., Hsinchu, Taiwan, Republic of China, 2011)
31. F Tosato, P Bisaglia, in *Proc. IEEE ICC 2002*. Simplified soft-output demapper for binary interleaved COFDM with application to HIPERLAN/2, (New York, USA, 2002), pp. 664–668
32. H Ochiai, H Imai, Performance analysis of deliberately clipped OFDM signals. IEEE Trans. Commun. **50**(1), 89–101 (2002)
33. N Seshadri, CEW Sundberg, List Viterbi decoding algorithms with applications. ITrans, EEE, Commun. **42**(234), 313–323 (1994)
34. L Bahl, J Cocke, F Jelinek, J Raviv, Optimal decoding of linear codes for minimizing symbol error rate (Corresp.) IEEE Trans. Inform. **20**(2), 284–287 (1974)
35. CW Tseng, YJ Wang, A 60 GHz 19.6 dBm power amplifier with 18.3 % PAE in 40 nm CMOS. IEEE Microwave Wireless Components Lett. **25**(2), 121-123 (2015)
36. D Zhao, P Reynaert, A 60-GHz dual-mode class AB power amplifier in 40-nm CMOS. IEEE J. Solid-State Circ. **48**(10), 2323–2337 (2013)
37. JP Kermoal, L Schumacher, PE Mogensen, Channel Characterization. IST-2000-30148 I-METRA-WP2-D2 (2002). http://www2.elo.utfsm.cl/~ipd465/Papers%20y%20apuntes%20varios/ISTinfo2000.pdf
38. AK Mustafa, S Ahmed, M Faulkner, Bandwidth limitation for the constant envelope components of an OFDM signal in a LINC architecture. IEEE Trans Circ. Syst I, Reg Papers. **60**(9), 2502–2510 (2013)
39. CD Chung, Correlatively coded OFDM. IEEE Trans Wireless Commun. **5**(8), 2044–2049 (2006)